Excited-State Dynamics of 3-Hydroxyflavone Anion in Alcohols
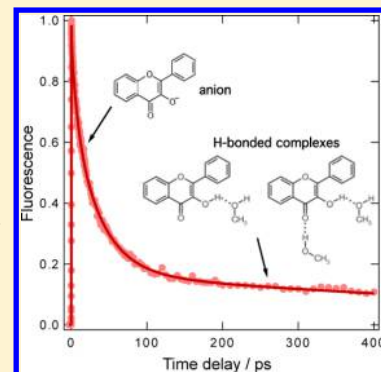
Bogdan Dereka,[†] Romain Letrun,[†] Denis Svechkarev,[†,‡] Arnulf Rosspeintner,[†] and Eric Vauthey[†,*]

[†]Department of Physical Chemistry, University of Geneva, 30 quai Ernest-Ansermet, CH-1211 Geneva 4, Switzerland
[‡]Institute of Chemistry, V.N. Karazin Kharkov National University, 4 Svobody Square, 61022 Kharkov, Ukraine

Ⓢ *Supporting Information*

ABSTRACT: The electronic absorption spectrum of 3-hydroxyflavone (3HF) in various solvents exhibits a long-wavelength (LW) band, whose origin has been debated. The excited-state dynamics of neutral and basic solutions of 3HF in alcohols upon excitation in this LW band has been investigated using a combination of fluorescence up-conversion and transient electronic and vibrational absorption spectroscopies. The ensemble of results reveals that, in neutral solutions, LW excitation results in the population of two excited species with similar fluorescence spectra but very different lifetimes, namely 40−100 ps and 2−3 ns, depending on the solvent. In basic solutions, the relative concentrations of these species change considerably in favor of that with the short-lived excited state. On the basis of the spectroscopic data and quantum chemistry calculations, the short lifetime is attributed to the excited state of 3HF anion, whereas the long one is tentatively assigned to an excited hydrogen-bonded complex with the solvent. Excited-state intermolecular proton transfer from the solvent to the anion yielding the tautomeric form of 3HF is not operative, as the excited anion decays to the ground state via an efficient nonradiative transition.

INTRODUCTION

Since the first report on the occurrence of excited-state intramolecular proton transfer (ESIPT) in 3-hydroxyflavone (3HF, Scheme 1A) by Sengupta and Kasha,[1] the photochemistry of flavonoids, and in particular that associated with proton transfer, has been intensively investigated. This includes studies in inert environments, such as supersonic molecular jets,[2,3] low temperature matrices,[4−6] helium nanodroplets,[7] and nonpolar media.[8] The ESIPT dynamics is well understood under those conditions: typically, excitation of 3HF results in a dual emission, with the weak normal fluorescence band around 400 nm and the more intense tautomeric band at longer wavelengths. The situation is more complicated in proton-donating or -accepting solvents, where solute−solvent interactions can substantially influence the structure of the molecule, via for example the formation of intermolecular H-bonds and/or the disruption of the H-bond, and thus modify its photochemistry.[9−11] Therefore, significant attention was focused on the different protic forms of 3HF as well as its H-bonded complexes with the solvent.[12−17] For example, several 3HF−methanol complexes have been suggested in ref 18. In some cases, the solvent disrupts the intramolecular H-bond that is directly involved in the ESIPT (a in Scheme 1B). An alcohol molecule could also form two H-bonds with 3HF, resulting in a chelate structure with a seven-membered ring (b in Scheme 1B), where solvent-mediated excited-state proton transfer should be favored.[18] On the other hand, in H-bond-accepting solvents, such as dimethylformamide (DMF), a new absorption band centered above 400 nm, i.e. at longer wavelength than that of the neutral 3HF, and called henceforth long-wavelength (LW) band is observed.[19] Optical excitation in this LW band leads to a new fluorescence band located between the normal

and tautomeric emission bands of 3HF. On the basis of the fluorescence spectrum recorded in the presence of a base, this emission was ascribed to the anion of 3HF originating from the transfer of the hydroxyl proton to the solvent or to H-bonded 3HF-solvent complexes (c and d in Scheme 1B).[19,20]

The 3HF anion was first characterized in basic water and methanol solutions by Wolfbeis et al.,[21] and later by Parthenopoulos and Kasha,[22] who also observed it in neutral formamide and reported an excited-state lifetime of 40 and 50 ps in basic methanol and neutral formamide, respectively. More recently, the anion was also detected in neutral alcohols by Mandal and Samanta, who reported a fluorescence lifetime of about 2 ns,[23] in agreement with that measured in neutral DMF.[19] In a subsequent investigation in solvents of varying H-bond-accepting and -donating strength, Protti et al. assigned the LW band and the associated fluorescence to a H-bonded anion−solvent complex rather than to the bare 3HF anion.[20]

Most of these studies of the anionic form of 3HF have concentrated on the mechanisms responsible for the presence of the LW band and have clearly shown they do not involve any excited-state process. We report here on our investigation of the excited-state dynamics of neutral and basic solutions of 3HF in methanol and ethanol upon LW excitation using a combination of ultrafast spectroscopic techniques. One of the motivations was to explore the possible formation of the
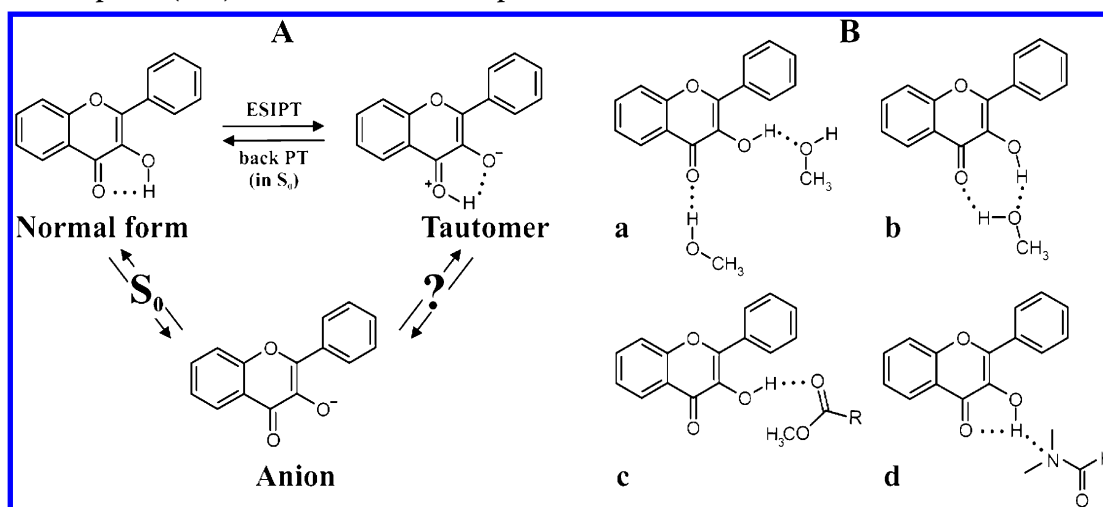
Scheme 1. (A) Normal, Tautomeric, and Anionic Forms of 3HF with Confirmed and Hypothetical Equilibria. (B) H-Bonded 3HF–Solvent Complexes (a–d) in Neutral Solution Proposed in Literature[18,19]

tautomeric form of 3HF upon excitation of the anion and subsequent proton transfer from the solvent. Our results show that such a process is not occurring or is at least not significant. However, they reveal that the LW absorption band is due to two species with similar emission spectra but with very different excited-state lifetimes, one of them being the anion and the other most probably a 3HF–solvent complex.

■ EXPERIMENTAL SECTION

Chemicals. 3-Hydroxyflavone (3HF) was purchased from Sigma-Aldrich and was used as received. The bases, sodium methoxide and sodium hydroxide, were of analytical grade and obtained from Acros Organics. The solvents methanol, methanol-d_4 (99.8 atom % D), and ethanol were of spectroscopic grade and purchased from either Sigma-Aldrich or Acros Organics.

Steady-State Spectroscopy. The absorption spectra were recorded with a Cary 50 spectrophotometer, whereas the emission spectra were measured with a Cary Eclipse (Varian) and a Horiba Fluoromax-4 (Jobin Yvon) spectrofluorimeter. Quartz cells with 1.00 and 10.00 mm path length were used for the measurements. All fluorescence spectra were corrected for the wavelength-dependent sensitivity of the detection and output of the excitation source. The fluorescence quantum yields were measured using coumarin 153 in ethanol as a reference ($\Phi_f = 0.38$).[24]

Time-Resolved Fluorescence. Fluorescence lifetime measurements on the nanosecond time scale were performed with a time-correlated single photon counting (TCSPC) setup described in detail elsewhere.[25,26] Excitation was carried out at 395 nm with a laser diode (Picoquant model LDH-P-C-400B) generating ~65 ps pulses at 20 MHz. The fluorescence was detected at magic angle with respect to the vertically polarized excitation. The samples, located in a 10 × 10 mm^2 quartz cell, had an absorbance of 0.1–0.3 at the excitation wavelength. The fluorescence time profiles were analyzed by iterative reconvolution of the instrument response function (IRF), recorded with a scattering LUDOX solution, with a sum of exponential functions. The IRF had a full width at half-maximum (fwhm) of about 200 ps.

The fluorescence dynamics on a shorter time scale was measured by fluorescence up-conversion (FU) with the setup

described in refs 27 and 28. Excitation was achieved at 400 nm with the frequency-doubled output of a Kerr lens mode-locked Ti:sapphire laser (Mai Tai, Spectra-Physics). The polarization of the pump pulses was at magic angle relative to that of the gate pulses at 800 nm. The pump intensity on the sample was of the order of 5 μJ·cm^{-2} and the fwhm of the IRF was ~210 fs. Neutral sample solutions were located in a rotating cell with 1.00 mm or 400 μm optical path length. Because of their limited photostability, the basic solutions were flowed in a 1.00 mm cell. Under this condition only, no photodegradation was observed during the measurements. The solutions had an absorbance between 0.03 and 0.4 at 400 nm.

Visible Transient Absorption (TA). The femtosecond visible TA setup has been described in detail elsewhere.[29,30] Excitation was performed at 400 nm with the frequency-doubled output of a standard 1 kHz amplified Ti:sapphire system (Spitfire, Spectra-Physics). The pump intensity on the sample was around 1 mJ·cm^{-2}. Probing was achieved with a white-light continuum obtained by focusing a small fraction of the 800 nm pulses on a CaF$_2$ plate. The polarization of the probe pulses was at magic angle relative to that of the pump pulses. All the spectra were corrected for the chirp of the white-light probe pulses. The fwhm of the IRF was ~200 fs. The neutral sample solutions were placed in a 1.00 mm quartz cell and were continuously stirred by N$_2$ bubbling, whereas the basic sample solutions were flowed through a 1.00 mm cell connected to a micro annular gear pump. Their absorbance at the excitation wavelength was between 0.03 and 0.5, depending on the sample.

Infrared Transient Absorption (IR-TA). The visible pump/mid-IR probe setup has been described in detail earlier.[31,32] Excitation was performed with 400 nm pulses generated by frequency doubling part of the output of a 1 kHz amplified Ti:sapphire system (Solstice, Spectra-Physics). The pump intensity on the sample was around 1 mJ·cm^{-2}. Probing was achieved with the output of an optical parametric amplifier (TOPAS-C, Light Conversion) connected to a difference-frequency mixing module (NDFG, Light Conversion) and polarized at magic angle relative to the pump pulses. Detection was performed with a 2 × 64 element MCT array (Infrared Systems Developments) connected with a spectrograph (Triax 190, 150 lines/mm, Horiba) resulting in a spectral resolution of

$1-2$ cm^{-1}. A flow cell as described in ref 33 was used. The absorbance of the sample at the excitation wavelength was below 0.5 on 100 μm.

Quantum Chemistry Calculations. Ground-state geometry optimization was performed at the density functional level of theory (DFT),[34] using the B3PW91 and B3LYP hybrid functionals and the 6-31G(d,p) and aug-N07D basis sets.[35,36] No symmetry or internal coordinate constraints were applied during optimization. Solvent effects were introduced via the polarized continuum model (PCM).[37] The calculations were performed using the Gaussian 09 package.[38]

■ RESULTS

Steady-State Spectroscopy. The electronic absorption spectrum of a solution of 3HF in methanol (Figure 1) or
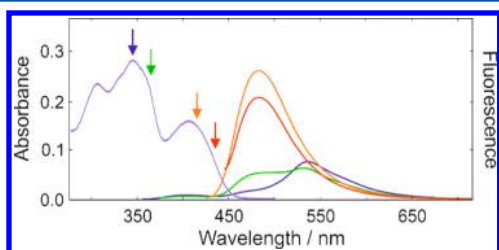

Figure 1. Electronic absorption and fluorescence spectra measured with a 10^{-4} M solution of 3HF in methanol. The excitation wavelengths used to record fluorescence are indicated by the colored arrows.

ethanol exhibits bands at 230, 305, and 345 nm that are characteristic of neutral 3HF as well as a weaker band centered at 415 nm, the LW band, that has been attributed to the anion or a 3HF–solvent complex.[19,20,23] The fluorescence spectra recorded with the same solutions vary substantially with the excitation wavelength (Figure 1). Upon 345 nm excitation, the spectrum consists of the weak normal band and the more intense tautomeric band of 3HF at 400 and 540 nm, respectively. A pronounced shoulder at 480 nm appears upon excitation at 365 nm, and its relative intensity increases upon increasing the excitation wavelength. Upon excitation in the LW band, the fluorescence spectrum exhibits a single band culminating at 480 nm that will be called the *LW-excited emission band*. The fluorescence quantum yield upon LW excitation amounts to 0.15 ± 0.01. These spectra are in full agreement with previous reports.[20–23] As the LW-excited emission band is relatively broad and overlaps with the tautomer emission band, the direct formation of the tautomeric form of 3HF upon LW excitation cannot be excluded, and time-resolved measurements are required to address this question.

Upon gradual addition of a base, either NaOH or CH$_3$ONa, to a methanol or ethanol solution of 3HF, the absorption bands of the neutral 3HF decrease, whereas the LW band increases and two isosbestic points can be observed (Figure 2A). These spectra indicate that the species responsible for the LW band also absorbs at shorter wavelengths. Therefore, selective photoexcitation of this species in the presence of 3HF is possible, but the opposite is not. A noticeable photodegradation of the solution takes place in the presence of a base already at equimolar concentration (10^{-4} M).

Addition of CH$_3$ONa has a substantial effect on the fluorescence spectrum as illustrated in Figure 2B. This base was chosen because, first, it is strong and readily deprotonates
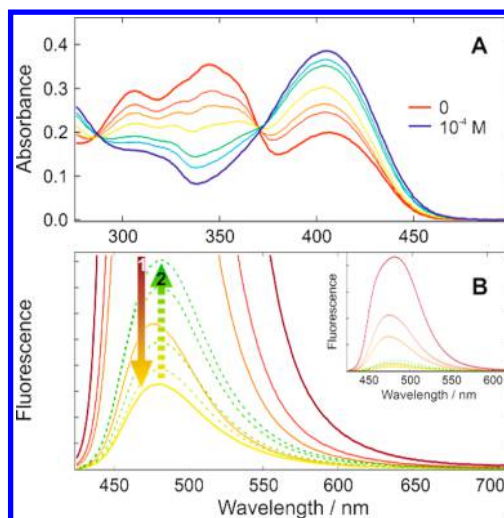

Figure 2. (A) Changes in the electronic absorption spectrum of a 10^{-4} M solution of 3HF in methanol upon addition of sodium methoxide up to an equimolar concentration. (B) Changes in the emission spectrum recorded with a solution of 3HF in methanol upon addition of sodium methoxide (arrow 1: from 0 to equimolar concentration (10^{-4} M); arrow 2: from 10^{-4} up to 7.5 × 10^{-3} M). The emission intensity was corrected for the changes of absorbance at 400 nm.

3HF and, second, it does not form water as a side product, which is one of the most powerful proton donors. However, no significant difference was noticed when using NaOH instead. At a base concentration of 7.5 × 10^{-5} M, i.e. smaller than that of 3HF (10^{-4} M), the fluorescence intensity decreases by a factor of 2, and keeps falling down to 10% of its initial intensity at 5.8 × 10^{-4} M. On the other hand, upon further addition of base up to 7.5 × 10^{-3} M, the fluorescence intensity increases by a factor of about 2.5.

Time-Resolved Fluorescence. The fluorescence dynamics upon LW excitation at 395 nm was first measured by TCSPC at three different wavelengths, namely 467, 532, and 575 nm. In principle, the tautomer fluorescence could contribute to the signal at 532 and 575 nm, but not at 467 nm. The fluorescence decays in neutral methanol solution are the same at all three wavelengths (Figure S1 in the Supporting Information [SI]). The sum of two exponential functions convolved with the IRF was required to properly reproduce these profiles, with time constants of 2.2 ns and 20 ps (Table 1). The latter time

Table 1. Time Constants and Relative Amplitudes (in brackets) Obtained from a Multiexponential Analysis of the Fluorescence Time Profiles Recorded by TCSPC at 467 nm with Solutions of 3HF at Different Base Concentrations, c

solvent, c(CH$_3$ONa)	τ_1/ns	τ_2/ns	τ_3/ns
methanol, 0 M	≪IRF (0.63)	2.2 (0.37)	
methanol, 10^{-4} M	≪IRF (0.96)	0.53 (0.03)	1.73 (0.02)
methanol, 10^{-3} M	≪IRF (0.87)	0.87 (0.08)	1.60 (0.05)
ethanol, 0 M	≪IRF (−0.38)	2.8 (1)	

constant is much shorter than the time resolution of the setup and was initially attributed to the well-known problem associated with the use of an IRF measured at a different wavelength.[39,40] However, as shown by the fluorescence up-conversion measurements discussed in detail below, an ultrafast decay component is indeed present. In ethanol, the decay is dominated by a 2.8 ns component, but it also required addition

of a component shorter than the IRF to be properly reproduced. The nanosecond lifetime agrees well with the values reported previously and attributed to the anion of 3HF.[19,23] As illustrated in Figure 3, a substantial acceleration of
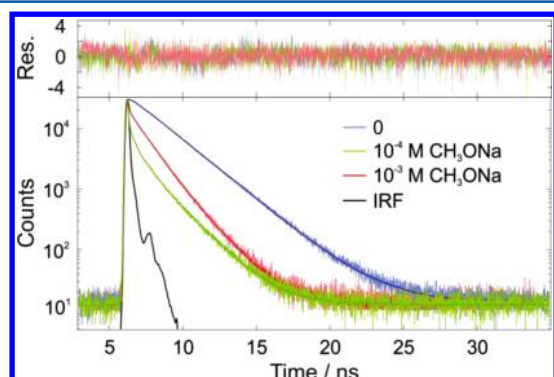

Figure 3. Intensity-normalized fluorescence decay profiles recorded at 467 nm with methanol solution of 3HF at various base concentrations, instrument response function (IRF), best fits (solid lines), and weighted residuals distribution (top).

the fluorescence dynamics takes place in the presence of 10^{-4} M CH_3ONa in the solution. In this case, the sum of three exponential functions was necessary to reproduce the data (Table 1 and Table S1 in the SI), more than 95% of the total amplitude being associated with a time constant much shorter than the IRF. Further addition of base leads to a slowing down of the dynamics in agreement with the observed increase of the fluorescence intensity.

No significant wavelength dependence was observed with any of the solutions investigated. This indicates that, if emission arises from different species, their fluorescence spectra are very similar. As a consequence, the formation of the tautomer of 3HF upon LW excitation can be ruled out.

FU measurements were carried out to resolve the faster components of the LW-excited fluorescence dynamics. FU profiles were recorded every 10−20 nm between 440 and 580 nm and up to 400 ps. Additionally to a significant wavelength dependence, Figure 4A reveals that, in neutral methanol, more than 50% of the initial amplitude decays in less than 50 ps. These profiles could be globally reproduced using the sum of four exponential functions with 0.33, 7.3, 36.0, and >400 ps time constants (Table 2) and the decay-associated spectra (DAS) depicted in Figure 4B. These best-fit parameters were then used to reconstruct time-resolved emission spectra (TRES),[41] the area-normalized ones being depicted in Figure 5A. Given the time window of these measurements, time constants larger than about 400 ps cannot be determined reliably. The 0.33 ps time constant is close to the IRF of the FU setup and some contribution of Raman scattering to the DAS, especially the 460 nm peak, could not be eliminated. The 0.33 and 7.3 ps DAS are positive at short wavelength and change sign above ∼480 nm. These DAS correspond to a red shift of the emission band, which is clearly visible in the TRES. Both time constants agree well with those reported for the solvation dynamics in methanol,[42,43] and consequently, they can be ascribed to the dynamic Stokes shift associated with solvent relaxation. This is comforted by similar measurements and analysis with 3HF in ethanol that yielded 0.6 and 11.6 ps time constants for the fastest components, in agreement with slower solvent relaxation dynamics (Table 2). The 36 and >400 ps
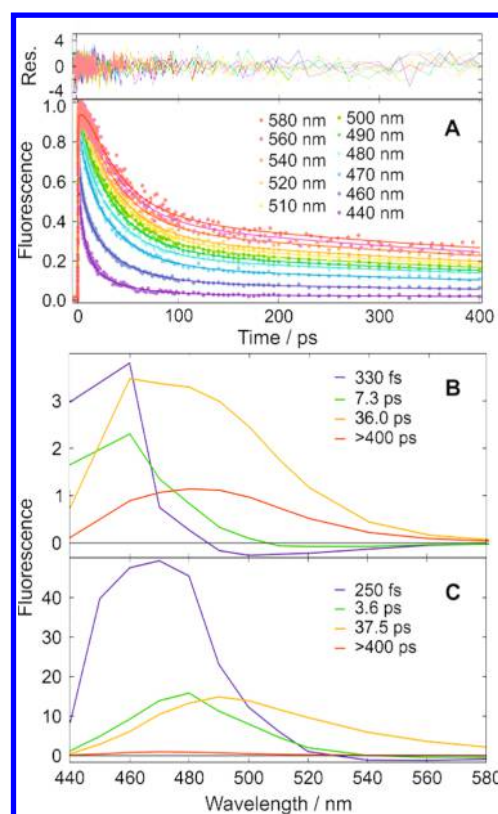

Figure 4. (A) Intensity-normalized fluorescence time profiles measured with a neutral solution of 3HF in methanol at various wavelengths. (B) Decay-associated spectra obtained from a global analysis of the time profiles in neutral and (C) basic (10^{-4} M CH_3ONa) methanol solutions of 3HF.

Table 2. Time Constants Obtained from a Multiexponential Global Analysis of the Fluorescence Time Profiles Measured by Fluorescence up-Conversion with Solutions of 3HF at Different Base Concentrations

solvent, $c(CH_3ONa)$	τ_1/ps	τ_2/ps	τ_3/ps	τ_4/ps
methanol, 0 M	0.33	7.3	36.0	>400
methanol, 10^{-4} M	0.25	3.6	37.5	>400
methanol, 10^{-3} M	0.32	4.4	44.1	>400
ethanol, 0 M	0.6	11.6	110	>400

DAS in methanol as well as the 110 and >400 ps DAS in ethanol are positive at all wavelengths (Figure 4B) and can thus be assigned to excited-state population decays. Their shapes are similar, but in a given solvent, the amplitude associated with the short time constant is about 3 times larger than that associated with the >400 ps time constant.

As no definite assignment is possible at the present stage, these emitting states will be called short-lived and long-lived excited states. It should nevertheless be noted that the 36 ps time constant found here in methanol agrees well with those of 50 and 40 ps reported by Parthenopoulos and Kasha in neutral formamide and basic methanol, respectively, and assigned to the excited-state lifetime of 3HF anion.[22]

Similar FU measurements were performed in methanol in the presence of equimolar concentration (10^{-4} M) of CH_3ONa, the time constants obtained from the multi-exponential global analysis being listed in Table 2 and the DAS and area-normalized TRES depicted in Figures 4C and 5B. Whereas the four time constants do not differ strongly from
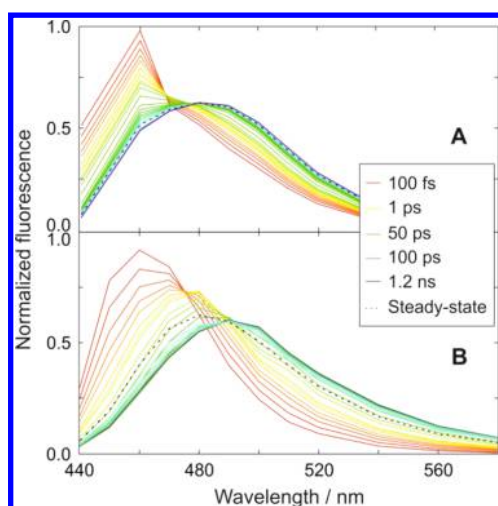
2437

dx.doi.org/10.1021/jp507311n | J. Phys. Chem. B 2015, 119, 2434−2443

Figure 5. (A) Area normalized time-resolved fluorescence spectra of neutral and (B) basic (10^{-4} M CH_3ONa) methanol solutions of 3HF and steady-state fluorescence spectrum (dashed line).

Figure 6. Electronic transient absorption spectra measured at various time delays after 400 nm excitation of a basic (10^{-4} M CH_3ONa) ethanol solution of 3HF.

those in neutral methanol and can be interpreted likewise, the DAS of the slowest component is much smaller, pointing to a negligible contribution of the long-lived excited-state to the overall dynamics. The situation is essentially the same with 10^{-3} M base (Figures S2, S3 in the SI).

The time-resolved fluorescence measurements reveal unambiguously that the LW-excited emission band in neutral methanol solution of 3HF originates from two different species. The >400 ps component obtained from FU corresponds to the nanosecond component observed in the TCSPC measurements.

From these time constants and the relative amplitudes of the DAS, one can conclude that more than 90% of the steady-state intensity of the LW-excited emission band is due to the long-lived excited state. In basic methanol, on the other hand, the long-lived excited state contributes to only a minor fraction of the steady-state fluorescence.

Visible and IR Transient Absorption. To obtain further insight into the excited-state dynamics upon LW excitation, visible transient absorption measurements have been performed with neutral and basic solutions of 3HF in methanol and ethanol. Because of the relative weakness of the LW band in neutral solutions, only small transient absorption signals ($\Delta A < 5 \times 10^{-3}$) could be measured. In general, the TA spectra measured in both alcohols were very similar, the only difference being a slower temporal evolution in ethanol. For this reason, only the TA spectra in the latter solvent will be presented here (Figure 6), those in methanol being shown in the SI (Figure S4). The early TA spectra are dominated by two positive bands around 460 and 560 nm and by a negative band at about 400 nm, which can be attributed to the bleach of the LW absorption and reflects the partial depletion of the ground-state population. A new negative band above 600 nm, hardly visible in neutral solutions, that can be assigned to stimulated emission, starts to develop after 0.5−1.5 ps, depending on the solvent. This change is accompanied by a decrease of the 560 nm band and a parallel increase of that at 460 nm, that is more marked in ethanol than in methanol. After a few tens of picoseconds, the spectral shape remains essentially unchanged, and the whole TA intensity decays to zero within less than 500 ps. In neutral methanol, a residual TA spectrum with a relative amplitude of a few percents can be observed until the longest time delay of the
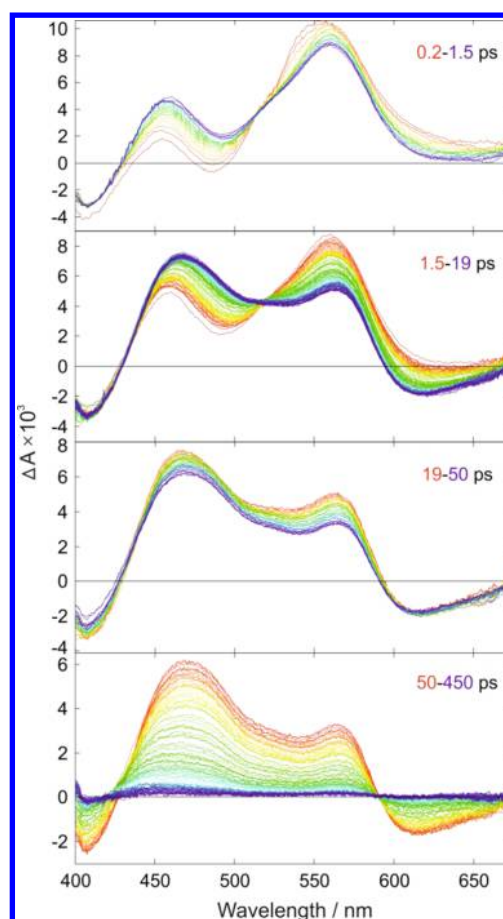
experiment. Its shape is mostly the same as that of the spectra measured after about 20 ps.

These transient spectra differ significantly from those reported for 3HF in neutral solutions upon excitation around 350 nm and attributed to the tautomeric form of 3HF, and consisting of two positive bands around 450 and 600 nm separated by a negative stimulated emission band at about 540 nm.[9,44]

The TA spectra were analyzed globally using both a sum of exponential functions and a target model consisting of a series of consecutive exponential steps.[45] The sum of three exponential functions and, thus, an A → B → C → D reaction scheme were sufficient to reproduce the observed dynamics of all samples, except neutral methanol, with the time constants listed in Table 3. In neutral methanol, an additional exponential function had to be added to account for the long-lived component. In general, these time constants agree well with those obtained from fluorescence measurements, the only difference being the absence of the long-lived components, except in neutral methanol. The longer time constant measured in the latter case could not be determined precisely, because of its small associated amplitude and the limited time window of the experiment. However, it most probably corresponds to the 2.2 ns lifetime measured by TCSPC. The species-associated difference spectra (SADS) obtained from the target analysis of the data measured with a basic ethanol solution are depicted in Figure 7, those for the methanol solution being presented in

Table 3. Time Constants Obtained from a Multiexponential Global Analysis of the Visible and IR Transient Absorption Data Recorded with Solutions of 3HF at Different Base Concentrations

solvent, $c(CH_3ONa)$	τ_1/ps	τ_2/ps	τ_3/ps	τ_4/ps
methanol, 0 M	0.4	5	40	~2000
methanol, 10^{-4} M	0.4	4.4 (4.2)[a]	44 (41)	
methanol-d_4, 10^{-4} M		4.3[a]	41[a]	
methanol, 10^{-3} M	0.3	4.1	49	
ethanol, 0 M	1.9	16	101	
ethanol, 10^{-4} M	1.0	13	95	
ethanol, 10^{-3} M	1.3	15	108	

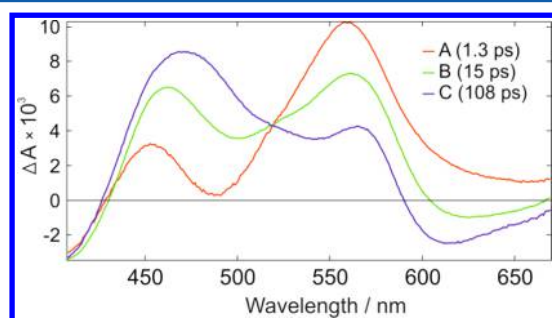[a]From IR transient absorption.

Figure 7. Species-associated difference spectra obtained from a target analysis of electronic transient absorption data measured with 3HF in basic ethanol (10^{-3} M CH$_3$ONa) assuming a A → B → C → D scheme.

Figure 8. Infrared transient absorption spectra measured at various time delays after 400 nm excitation of basic (10^{-4} M CH$_3$ONa) methanol-d_4 solution of 3HF. The steady-state FTIR spectrum (purple) as well as the frequencies and oscillator strengths (vertical bars) calculated at the B3LYP/aug-N07D level of theory are also shown.

Figure S5 in the SI. They differ mainly by the position and amplitude of the dip separating the two positive TA bands and of the negative band above 600 nm. The dip shifts to longer wavelengths and weakens when going from A to B and to C, whereas the >600 nm band becomes more negative. Comparison with the FU measurements (Figure 5) indicates that these changes can be accounted for by the dynamic Stokes shift of the stimulated emission band. Stimulated emission overlaps with a positive TA band resulting in the dip and the appearance of two positive bands. As solvent relaxation takes place, the dip shifts to longer wavelengths and the negative band above 600 nm becomes more intense. As a consequence, species A and B can be assigned to the unrelaxed and partially relaxed excited state populated upon LW excitation, and species C to the equilibrated excited state.

These TA measurements reveal that the long-lived excited state that is responsible for most of the LW fluorescence in neutral methanol represents only a minor fraction, a few percents, of the overall excited-state population. In basic solutions, this fraction is too small to significantly contribute to the TA signal. No conclusion on the exact nature of the short-lived excited state populated upon LW excitation can be drawn from these transient electronic spectra. However, the recovery of the ground-state population indicates that its main decay pathway is internal conversion to the ground state.

To get more structural information, IR−TA measurements have been performed with a basic solution of 3HF in methanol and methanol-d_4. The minimum sample absorbance required to perform such measurements could not be achieved with neutral solutions. Figure 8 shows IR−TA spectra recorded at various time delays after LW excitation in methanol-d_4 in the 1500−1750 cm^{-1} spectral window, where absorption due to the
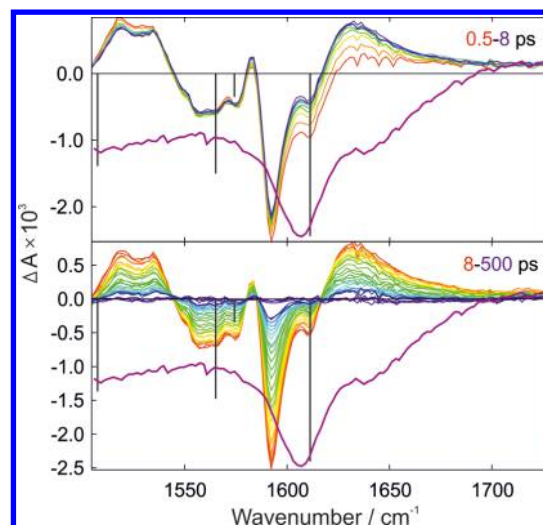
carbonyl stretching mode is expected. The earliest TA spectra exhibit two negative bands, a sharp and intense at 1592 cm^{-1} with a sideband at 1610 cm^{-1} and a broad and relatively weaker one around 1560 cm^{-1}, and one positive band centered at about 1526 cm^{-1}. During the first 8 ps, the intensity of these bands decreases by approximately 10%, while a new broad positive band develops around 1630 cm^{-1}. From about 8 ps onward, the overall shape of the TA spectra remains constant, and the intensity of all features decays to zero within 200 ps. The IR−TA spectra in methanol exhibit the same features within ±1 cm^{-1} (Figure S6 in the SI). The stationary IR absorption spectrum measured with the same solution is dominated by a band at 1610 cm^{-1} (Figure 8), which is upshifted by about 20 cm^{-1} relative to the intense negative TA band, but coincides with the 1610 cm^{-1} sideband. This shift can be explained by the presence of an excited-state TA feature overlapping with the ground-state bleach.

These spectra differ substantially from those reported for 3HF in acetonitrile upon 360 nm excitation,[44] which exhibit two negative bands, at 1623 and 1575 cm^{-1}, and a broad positive feature centered around 1520 cm^{-1}. The frequencies of the negative bands were shown to agree well with those obtained from quantum chemistry calculations of 3HF in the ground state.[44]

On the other hand, Figure 8 also reveals that the calculated IR frequencies of 3HF anion in methanol obtained from DFT calculations at the B3LYP/aug-N07D level of theory match the experimental spectra very well. The calculated vibration frequencies were scaled by a factor of 0.9613, that has been shown to be adequate when using the B3LYP functional.[46] These calculations predict the carbonyl stretching band at 1610 cm^{-1}, and a band due to a combination of C=O and C=C modes at 1570 cm^{-1}. This excellent agreement points unambiguously to the anion of 3HF as the main species responsible for the LW absorption band in basic solution.

The time evolution of the TA spectra could be reproduced globally using the sum of two exponential functions with time constants of 4.3 and 41 ps and the decay-associated difference

2439

dx.doi.org/10.1021/jp507311n | J. Phys. Chem. B 2015, 119, 2434−2443

spectra depicted in Figure S7 in the SI. Both time constants are in excellent agreement with those obtained from the electronic TA and FU measurements and are ascribed to solvent relaxation and decay of the short-lived excited state, respectively. The subpicosecond component was not observed in the IR–TA measurements since it is close to the instrument response function. The broad positive TA feature at around 1630 cm^{-1} can be ascribed to the C=O stretching mode of the excited state. This is most probably not the entire band but only its high frequency edge, as the main part overlaps with the bleach of the 1610 cm^{-1} ground-state band.

An upshift of the C=O stretch frequency upon photoexcitation has already been reported with other chromophores containing carbonyl groups.[47,48] The excited-state C=O band was also shown to increase and further shift to high frequencies upon solvent relaxation.[49] The rise of this 1630 cm^{-1} feature with the 4.3 ps component is fully compatible with solvent relaxation. This rise is most probably due to the shift of the excited-state C=O band, which is overlapping with the 1610 cm^{-1} bleach. This also explains why the 1610 cm^{-1} sideband decreases by a factor 2 during the first 8 ps, whereas the intensity of the band maximum at 1593 cm^{-1} changes by only about 10%.

■ DISCUSSION

All the time-resolved spectroscopic data point unambiguously to the existence of two species responsible for the LW absorption band of neutral methanol and ethanol solutions of 3HF, which differ by their excited-state lifetime, 40–100 ps and 2–3 ns depending on the solvent. The short-lived excited state accounts for approximately 2/3 of the initial fluorescence intensity, but only for about 1/10 of the integrated fluorescence intensity. The electronic TA measurements indicate that more than 90% of the total ground-state population recovers with the shorter time constant. This difference in the contribution of the two species to the signal amplitude points to a radiative rate constant of the long-lived species larger than that of the short-lived one.

Addition of a base to the solution leads to an increase of the LW intensity and a concomitant decrease of the LW-excited fluorescence intensity. The latter is due to an almost complete disappearance of the species with the long-lived excited state. The fact that mostly the amplitude but not so much the lifetime of the long-lived component is affected by the base indicates that the disappearance of the long-lived component is not due to an excited-state quenching process but rather to an effect of the base on the ground-state populations. The visible TA measurements do not allow identification of these species. Nevertheless, the substantial dynamic Stokes shift observed in both FU and visible TA measurements is a clear indication that the species with the short-lived excited state undergoes a substantial change in electronic distribution upon photoexcitation. Furthermore, IR–TA measurements reveal that both the dynamics and frequency of the transient bands are independent of the deuteration of the solvent, suggesting that this species is not H-bonded to the solvent.

The species with the short-lived excited state can be undoubtedly interpreted as the anion of 3HF. First, the relative concentration of 3HF anion should increase upon addition of a base, as observed. Second, the calculated IR absorption spectrum of the 3HF anion matches very well the stationary and transient spectra measured in the 1500–1750 cm^{-1} region. Third, TD-DFT calcul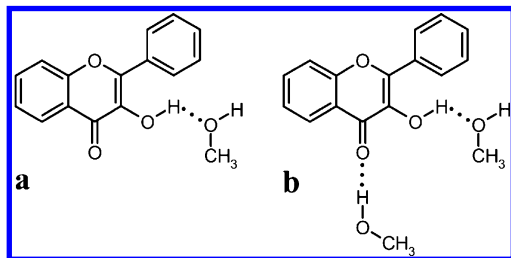ations indicate that the first singlet electronic excited state of 3HF anion originates from a one-electron HOMO–LUMO transition, which, as shown in Figure S8 in the SI, involves a substantial redistribution of the electronic density, in agreement with the observed dynamic Stokes shift of the fluorescence. Fourth, the absence of the kinetic isotope effect on the excited-state dynamics and on the IR spectrum suggests that this species is not a 3HF–solvent complex. This assignment agrees with that of Parthenopoulos and Kasha, who also ascribed the transient species with 40 and 50 ps lifetime observed in basic methanol and neutral formamide to the excited 3HF anion.[22]

The previous assignments of the ~2 ns component to the anion can be explained by the fact that (i) the fast decaying component in methanol is not visible when using TCSPC with an IRF of ≥200 ps,[23] and (ii) in FU measurements upon 371 nm excitation,[19] the relative absorbance of the anion at that wavelength is so small that its fluorescence is completely hidden by that of the 3HF tautomer and only the weak long-lived residual is visible.

The reason for the short excited-state lifetime of 3HF anion still remains to be clarified. The TA measurements show unambiguously that the excited state of the anion decays nonradiatively to the ground state and is not converted into another excited state, such as a triplet state or the tautomeric form of neutral 3HF. H-bond-assisted nonradiative deactivation, as observed with several chromophores possessing H-bond-accepting groups,[50−55] could explain the increased lifetime measured when going from methanol to ethanol, i.e. when decreasing the H-bond-donating strength of the solvent. However, the absence of a kinetic isotope effect does not support this mechanism. A nonradiative mechanism involving large amplitude motion could also explain the longer lifetime in ethanol that is about twice as viscous as methanol. However, with molecules of similar size, such process is normally faster, taking place in a few picoseconds in solvents of viscosity similar to that of methanol,[31,56−58] unless it involves a barrier in addition to that associated with friction.[59−61] Further measurements in solvents of varying viscosity and/or at different temperatures would be necessary to evidence such process. However, the poor photostability of the basic solutions of 3HF is a serious limitation. High-level quantum chemistry calculations of the potential energy surface of the ground and excited states of the anion could be an alternative approach.[62−66]

The various experimental data described above do not allow the species responsible for the 2−3 ns component to be identified. As it has been observed independently by many groups, this species cannot be ascribed to an impurity, but coexists with the anion of 3HF in neutral solutions. Furthermore, the resemblance of its emission spectrum with that of the anion points to a similar electronic structure. This species is most probably a 3HF–solvent complex with the hydroxyl group of 3HF H-bonded to the solvent, as already suggested in previous studies.[18−20] This is supported by an abrupt decrease of the contribution of this component upon addition of the base, since the equilibrium between this complex and the anion is displaced toward the latter. The binding to the solvent increases the electronic density on the hydroxyl oxygen atom and results in some anionic character. Although no exact structure can be proposed for this complex, it should be such that it does not allow intramolecular H-bonding and, thus, prevents ESIPT, like those illustrated in Scheme 2. Support from quantum chemical calculations would

Scheme 2. Hypothetical Structures of the H-Bonded 3HF–Solvent Complexes Responsible for the Long Fluorescence Lifetime in Neutral Alcohol Solutions of 3HF

require an explicit treatment of the methanol molecules surrounding 3HF to properly account for the H-bond network. However, such calculations go far beyond the main scope of the present investigation.

CONCLUDING REMARKS

Our investigation reveals that the origin of the LW electronic absorption band measured with solutions of 3HF in alcohols is more complicated than previously assumed and explains the very divergent excited-state lifetimes of the 3HF anion reported in literature. This LW band is due to the presence of two species, most probably in equilibrium, that are characterized by similar fluorescence spectra but very distinct excited-state lifetimes, around 40–100 ps and 2–3 ns, depending on the solvent. As the relative concentration of the species with the short lifetime increases and becomes dominant upon addition of a base, it is ascribed to the anion of 3HF. This assignment is also supported by the excellent agreement between the spectroscopic data and the quantum chemistry calculations. Most of the fluorescence measured in neutral solution upon LW excitation arises from the species with a 2–3 ns excited-state lifetime. The nature of this species is still not obvious, but it is most probably an H-bonded complex of the neutral 3HF with the solvent. In any case, our investigation shows unambiguously that excited-state proton transfer upon excitation of either of these species is not operative.

ASSOCIATED CONTENT

Ⓢ Supporting Information

Additional spectroscopic data (TCSPC, time-resolved emission spectra, electronic and infrared transient absorption spectra, species- and decay-associated spectra), frontier molecular orbitals of 3HF anion, and best-fit parameters obtained from the analysis of TCSPC data. This material is available free of charge via the Internet at http://pubs.acs.org.

AUTHOR INFORMATION

Corresponding Author
*E-mail: eric.vauthey@unige.ch

Notes
The authors declare no competing financial interest.

ACKNOWLEDGMENTS

REFERENCES

(1) Sengupta, P. K.; Kasha, M. Excited State Proton-Transfer Spectroscopy of 3-Hydroxyflavone and Quercetin. *Chem. Phys. Lett.* **1979**, *68*, 382−385.

(2) Bartl, K.; Funk, A.; Schwing, K.; Fricke, H.; Kock, G.; Martin, H.-D.; Gerhards, M. IR Spectroscopy Applied Subsequent to a Proton Transfer Reaction in the Excited State of Isolated 3-Hydroxyflavone and 2-(2-Naphthyl)-3-hydroxychromone. *Chem. Phys. Phys. Chem.* **2009**, *11*, 1173−1179.

(3) Ernsting, N. P.; Dick, B. Fluorescence Excitation of Isolated, Jet-Cooled 3-Hydroxyflavone: The Rate of Excited State Intramolecular Proton Transfer from Homogeneous Linewidths. *Chem. Phys.* **1989**, *136*, 181−186.

(4) Brucker, G. A.; Kelley, D. F. Proton Transfer in Matrix-Isolated 3-Hydroxyflavone and 3-Hydroxyflavone Complexes. *J. Phys. Chem.* **1987**, *91*, 2856−2861.

(5) Brucker, G. A.; Kelley, D. F. Role of Phenyl Torsion in the Excited-State Dynamics of 3-Hydroxyflavone. *J. Phys. Chem.* **1988**, *92*, 3805−3809.

(6) Bader, A. N.; Ariese, F.; Gooijer, C. Proton Transfer in 3-Hydroxyflavone Studied by High-Resolution 10 K Laser-Excited Shpol'skii Spectroscopy. *J. Phys. Chem. A* **2002**, *106*, 2844−2849.

(7) Lehnig, R.; Pentlehner, D.; Vdovin, A.; Dick, B.; Slenczka, A. Photochemistry of 3-Hydroxyflavone inside Superfluid Helium Nanodroplets. *J. Chem. Phys.* **2009**, *131*, 194307.

(8) McMorrow, D.; Kasha, M. Intramolecular Excited-State Proton Transfer in 3-Hydroxyflavone. Hydrogen-Bonding Solvent Perturbations. *J. Phys. Chem.* **1984**, *88*, 2235−2243.

(9) Ameer-Beg, S.; Ormson, S. M.; Brown, R. G.; Matousek, P.; Towrie, M.; Nibbering, E. T. J.; Foggi, P.; Neuwahl, F. V. R. Ultrafast Measurements of Excited State Intramolecular Proton Transfer (ESIPT) in Room Temperature Solutions of 3-Hydroxyflavone and Derivatives. *J. Phys. Chem. A* **2001**, *105*, 3709−3718.

(10) Schwartz, B. J.; Peteanu, L. A.; Harris, C. B. Direct Observation of Fast Proton Transfer: Femtosecond Photophysics of 3-Hydroxy-flavone. *J. Phys. Chem.* **1992**, *96*, 3591−3598.

(11) Sytnik, A.; Gormin, D.; Kasha, M. Interplay between Excited-State Intramolecular Proton Transfer and Charge Transfer in Flavonols and their Use as Protein-Binding-Site Fluorescence Probes. *Proc. Natl. Acad. Sci. U.S.A.* **1994**, *91*, 11968−11972.

(12) Sytnik, A.; Litvinyuk, I. Energy Transfer to a Proton-Transfer Fluorescence Probe: Tryptophan to a Flavonol in Human Serum Albumin. *Proc. Natl. Acad. Sci. U.S.A.* **1996**, *93*, 12959−12963.

(13) Guharay, J.; Sengupta, B.; Sengupta, P. K. Protein-Flavonol Interaction: Fluorescence Spectroscopic Study. *Proteins* **2001**, *43*, 75−81.

(14) Shyamala, T.; Mishra, A. K. Ground- and Excited-State Proton Transfer Reaction of 3-Hydroxyflavone in Dimyristoylphosphatidyl-choline Liposome Membrane. *Photochem. Photobiol.* **2004**, *80*, 309−315.

(15) Mohapatra, M.; Subuddhi, U.; Mishra, A. K. Photophysical Behaviour of Ground State Anion and Phototautomer of 3-Hydroxyflavone in Liposome Membrane. *Photochem. Photobiol. Sci.* **2009**, *8*, 1373−1378.

(16) Tormo, L.; Douhal, A. Caging Anionic Structure of a Proton Transfer Dye in a Hydrophobic Nanocavity with a Cooperative H-bonding. *J. Photochem. Photobiol., A* **2005**, *173*, 358−364.

(17) Yushchenko, D.; Vadzyuk, O. B.; Kosterin, S. O.; Duportail, G.; Mély, Y.; Pivovarenko, V. G. Sensing of Adenosine-5′-Triphosphate Anion in Aqueous Solutions and Mitochondria by a Fluorescent 3-Hydroxyflavone Dye. *Anal. Biochem.* **2007**, *369*, 218−225.

(18) Woolfe, G. J.; Thistlethwaite, P. J. Direct Observation of Excited State Intramolecular Proton Transfer Kinetics in 3-Hydroxyflavone. *J. Am. Chem. Soc.* **1981**, *103*, 6916−6923.

(19) Douhal, A.; Sanz, M.; Tormo, L.; Organero, J. A. Femtochemistry of Inter- and Intramolecular Hydrogen Bonds. *ChemPhysChem* **2005**, *6*, 419−423.

(20) Protti, S.; Mezzetti, A.; Cornard, J.-P.; Lapouge, C.; Fagnoni, M. Hydrogen Bonding Properties of DMSO in Ground-State Formation

and Optical Spectra of 3-Hydroxyflavone Anion. *Chem. Phys. Lett.* **2008**, *467*, 88−93.

(21) Wolfbeis, O. S.; Knierzinger, A.; Schipfer, R. pH-Dependent Fluorescence Spectroscopy XVII: First Excited Singlet State Dissociation Constants, Phototautomerism and Dual Fluorescence of Flavonol. *J. Photochem.* **1983**, *21*, 67−79.

(22) Parthenopoulos, D. a.; Kasha, M. Ground State Anion Formation and Picosecond Excitation Dynamics of 3-Hydroxyflavone in Formamide. *Chem. Phys. Lett.* **1990**, *173*, 303−309.

(23) Mandal, P. K.; Samanta, A. Evidence of Ground-State Proton-Transfer Reaction of 3-Hydroxyflavone in Neutral Alcoholic Solvents. *J. Phys. Chem. A* **2003**, *107*, 6334−6339.

(24) Jones, G.; Jackson, W. R.; Choi, C. Y.; Bergmark, W. R. Solvent Effects on Emission Yield and Lifetime for Coumarin Laser Dyes. Requirements for a Rotatory Decay Mechanism. *J. Phys. Chem.* **1985**, *89*, 294−300.

(25) Muller, P.-A.; Högemann, C.; Allonas, X.; Jacques, P.; Vauthey, E. Deuterium Isotope Effect on the Charge Recombination Dynamics of Contact Ion Pairs Formed by Electron Transfer Quenching in Acetonitrile. *Chem. Phys. Lett.* **2000**, *326*, 321−327.

(26) Fürstenberg, A.; Vauthey, E. Ultrafast Excited-State Dynamics of Oxazole Yellow DNA Intercalators. *J. Phys. Chem. B* **2007**, *111*, 12610−12620.

(27) Morandeira, A.; Engeli, L.; Vauthey, E. Ultrafast Charge Recombination of Photogenerated Ion Pairs to an Electronic Excited State. *J. Phys. Chem. A* **2002**, *106*, 4833−4837.

(28) Duvanel, G.; Grilj, J.; Chaumeil, H.; Jacques, P.; Vauthey, E. Ultrafast Excited-State Dynamics of a Series of Zwitterionic Pyridinium Phenoxides with Increasing Sterical Hindering. *Photochem. Photobiol. Sci.* **2010**, *9*, 908−915.

(29) Duvanel, G.; Banerji, N.; Vauthey, E. Excited-State Dynamics of Donor-Acceptor Bridged Systems Containing a Boron-Dipyrromethene Chromophore: Interplay between Charge Separation and Reorientational Motion. *J. Phys. Chem. A* **2007**, *111*, 5361−5369.

(30) Banerji, N.; Duvanel, G.; Perez-Velasco, A.; Maity, S.; Sakai, N.; Matile, S.; Vauthey, E. Excited-State Dynamics of Hybrid Multichromophoric Systems: Toward an Excitation Wavelength Control of the Charge Separation Pathways. *J. Phys. Chem. A* **2009**, *113*, 8202−8212.

(31) Letrun, R.; Koch, M.; Dekhtyar, M. L.; Kurdyukov, V. V.; Tolmachev, A. I.; Rettig, W.; Vauthey, E. Ultrafast Excited-State Dynamics of Donor−Acceptor Biaryls: Comparison between Pyridinium and Pyrylium Phenolates. *J. Phys. Chem. A* **2013**, *117*, 13112−13126.

(32) Koch, M.; Letrun, R.; Vauthey, E. Exciplex Formation in Bimolecular Photoinduced Electron-Transfer Investigated by Ultrafast Time-Resolved Infrared Spectroscopy. *J. Am. Chem. Soc.* **2014**, *136*, 4066−4074.

(33) Bredenbeck, J.; Hamm, P. Versatile Small Volume Closed-Cycle Flow Cell System for Transient Spectroscopy at High Repetition Rates. *Rev. Sci. Instrum.* **2003**, *74*, 3188−3189.

(34) Kohn, W.; Sham, L. J. Self-Consistent Equations Including Exchange and Correlation Effects. *Phys. Rev.* **1965**, *140*, A1133−A1138.

(35) Barone, V.; Cimino, P.; Stendardo, E. Development and Validation of the B3LYP/N07D Computational Model for Structural Parameter and Magnetic Tensors of Large Free Radicals. *J. Chem. Theory Comput.* **2008**, *4*, 751−764.

(36) Puzzarini, C.; Biczysko, M.; Barone, V. Accurate Anharmonic Vibrational Frequencies for Uracil: The Performance of Composite Schemes and Hybrid CC/DFT Model. *J. Chem. Theory Comput.* **2011**, *7*, 3702−3710.

(37) Cossi, M.; Scalmani, G.; Rega, N.; Barone, V. New Developments in the Polarizable Continuum Model for Quantum Mechanical and Classical Calculations on Molecules in Solution. *J. Chem. Phys.* **2002**, *117*, 43−54.

(38) Frisch, M. J., et al. *Gaussian 09*, revision C1; Gaussian, Inc.: Wallingford, CT, 2010.

(39) Van Den Zegel, M.; Boens, N.; Daems, D.; De Schryver, F. C. Possibilities and Limitations of the Time-Correlated Single Photon Counting Technique: a Comparative Study of Correction Methods for the Wavelength Dependence of the Instrument Response Function. *Chem. Phys.* **1986**, *101*, 311−335.

(40) Kolber, Z. S.; Barkley, M. D. Comparison of Approaches to the Instrumental Response Function in Fluorescence Decay Measurements. *Anal. Biochem.* **1986**, *152*, 6−21.

(41) Fürstenberg, A.; Julliard, M. D.; Deligeorgiev, T. G.; Gadjev, N. I.; Vassilev, A. A.; Vauthey, E. Ultrafast Excited-State Dynamics of DNA Fluorescent Intercalators: New Insight into the Fluorescence Enhancement Mechanism. *J. Am. Chem. Soc.* **2006**, *128*, 7661−7669.

(42) Horng, M. L.; Gardecki, J. A.; Papazyan, A.; Maroncelli, M. Subpicosecond Measurements of Polar Solvation Dynamics: Coumarin 153 Revisited. *J. Phys. Chem.* **1995**, *99*, 17311−17337.

(43) Gumy, J. C.; Nicolet, O.; Vauthey, E. Investigation of the Solvation Dynamics of an Organic Dye in Polar Solvents Using the Femtosecond Transient Grating Technique. *J. Phys. Chem. A* **1999**, *103*, 10737−10743.

(44) Chevalier, K.; Wolf, M. M. N.; Funk, A.; Andres, M.; Gerhards, M.; Diller, R. Transient IR Spectroscopy and Ab Initio Calculations on ESIPT in 3-Hydroxyflavone Solvated in Acetonitrile. *Phys. Chem. Chem. Phys.* **2012**, *14*, 15007−15020.

(45) van Stokkum, I. H. M.; Larsen, D. S.; van Grondelle, R. Global and Target Analysis of Time-Resolved Spectra. *Biochim. Biophys. Acta, Bioenerg.* **2004**, *1657*, 82−104.

(46) Wong, M. W. Vibrational Frequency Prediction Using Density Functional Theory. *Chem. Phys. Lett.* **1996**, *256*, 391−399.

(47) Nibbering, E. T. J.; Fidder, H.; Pines, E. Ultrafast Chemistry: Using Time-Resolved Vibrational Spectroscopy for Interrogation of Structural Dynamics. *Annu. Rev. Phys. Chem.* **2005**, *56*, 337−367.

(48) Zhao, G.-J.; Han, K.-L. Hydrogen Bonding in the Electronic Excited State. *Acc. Chem. Res.* **2011**, *45*, 404−413.

(49) Nibbering, E. T. J.; Tschirschwitz, F.; Chudoba, C.; Elsaesser, T. Femtochemistry of Hydrogen Bonded Complexes after Electronic Excitation in the Liquid Phase: The Case of Coumarin 102. *J. Phys. Chem. A* **2000**, *104*, 4236−4246.

(50) Flom, S. R.; Barbara, P. F. Proton Transfer and Hydrogen Bonding in the Internal Conversion of S1 Anthraquinones. *J. Phys. Chem.* **1985**, *89*, 4489−4494.

(51) Inoue, H.; Hida, M.; Nakashima, N.; Yoshihara, K. Picosecond Fluorescence Lifetimes of Anthraquinone Derivatives. Radiationless Deactivation via Intra- and Intermolecular Hydrogen Bonds. *J. Phys. Chem.* **1982**, *86*, 3184−3188.

(52) Mohammed, O. F.; Vauthey, E. Excited-State Dynamics of Nitroperylene in Solution: Solvent and Excitation Wavelength Dependence. *J. Phys. Chem. A* **2008**, *112*, 3823−3830.

(53) Sherin, P. S.; Grilj, J.; Tsentalovitch, Y. P.; Vauthey, E. Ultrafast Excited-State Dynamics of Kynurenine, a UV Filter of the Human Eye. *J. Phys. Chem. B* **2009**, *113*, 4953−4962.

(54) Petkova, I.; Dobrikov, G.; Banerji, N.; Duvanel, G.; Perez, R.; Dimitrov, D.; Nikolov, P.; Vauthey, E. Tuning the Excited-State Dynamics of GFP-Inspired Imidazolone Derivatives. *J. Phys. Chem. A* **2010**, *114*, 10−20.

(55) Fita, P.; Fedoseeva, M.; Vauthey, E. Ultrafast Excited-State Dynamics of Eosin B: a Potential Probe of the Hydrogen-Bonding Properties of the Environment. *J. Phys. Chem. A* **2011**, *115*, 2465−2470.

(56) Aberg, U.; Akesson, E.; Sundström, V. Excited State Dynamics of Barrierless Isomerization in Solution. *Chem. Phys. Lett.* **1993**, *215*, 388−394.

(57) Todd, D. C.; Jean, J. M.; Rosenthal, S. J.; Ruggiero, A. J.; Yang, D.; Fleming, G. R. Fluorescence Upconversion Study of cis-Stilbene Isomerization. *J. Chem. Phys.* **1990**, *93*, 8658−8668.

(58) Litvinenko, K. L.; Webber, N. M.; Meech, S. R. Internal Conversion in the Chromophore of the Green Fluorescent Protein: Temperature Dependence and Isoviscosity Analysis. *J. Phys. Chem. A* **2003**, *107*, 2616−2623.

2442

dx.doi.org/10.1021/jp507311n | *J. Phys. Chem. B* 2015, 119, 2434−2443

(59) Sivakumar, N.; Hoburg, E. A.; Waldeck, D. H. Solvent Dielectric Effects on Isomerisation Dynamics: Investigation of the Photoisomerisation of 4,4′-Dimethoxystilbene and t-Stilbene in n-Alkyl Nitriles. *J. Chem. Phys.* **1989**, *90*, 2305−2316.

(60) Saltiel, J.; Waller, A. S.; S, D. F., Jr.; Hoburg, E. A.; Zeglinski, D. M.; H.Waldeck, D. Fluorescence Quantum Yields and Lifetimes of Substituted Stilbenes in n-Alkanes. A Reexamination of the Relationship between Solute Size and Medium Effect on Torsional Relaxation. *J. Phys. Chem.* **1994**, *98*, 10689−10698.

(61) Vauthey, E. Isomerisation Dynamics of a Thiacarbocyanine Dye in Different Electronic States and in Different Classes of Solvents. *Chem. Phys.* **1995**, *196*, 569−582.

(62) Grilj, J.; Laricheva, E. N.; Olivucci, M.; Vauthey, E. Fluorescence of Radical Ions in Liquid Solution: Wurster's Blue as a Case Study. *Angew. Chem., Int. Ed.* **2011**, *50*, 4496−4498.

(63) Ismail, N.; Blancafort, L.; Olivucci, M.; Kohler, B.; Robb, M. A. Ultrafast Decay of Electronically Excited Singlet Cytosine via a π,π^* to n,π^* State Switch. *J. Am. Chem. Soc.* **2002**, *124*, 6818−6819.

(64) Quenneville, J.; Martínez, T. J. Ab Initio Study of Cis−Trans Photoisomerization in Stilbene and Ethylene. *J. Phys. Chem. A* **2003**, *107*, 829−837.

(65) Levine, B. G.; Martinez, T. J. Isomerization through Conical Intersections. *Annu. Rev. Phys. Chem.* **2006**, *58*, 613−634.

(66) Hunt, P. A.; Robb, M. A. Systematic Control of Photochemistry: The Dynamics of Photoisomerization of a Model Cyanine Dye. *J. Am. Chem. Soc.* **2005**, *127*, 5720−5726.